PROTON AND ELECTRON AURORA OVER EISCAT:
OPTICAL SIGNATURE AND ASSOCIATED IONOSPHERIC PERTURBATIONS

M. Galand(1), J. Baumgardner(1), S. Chakrabarti (1),
U. P. Løvhaug(2), B. Isham(3), J. Jussila(4), D. Evans(5), F. Rich(6), D. Lummerzheim(7)
(1) Center for Space Physics, Boston University, 725 Commonwealth Avenue, Boston, MA 02215, USA,
Email: mgaland@bu.edu, jeffreyb@bu.edu, supc@bu.edu
(2) Department of Physics, University of Tromsø, Tromsø, N-9037, Norway, Unni.Pia.Lovhaug@phys.uit.no
(3) EISCAT Scientific Association, Ramfjordmoen, Ramfjordbotn, NO-9027, Norway, isham@eiscat.uit.no
(4) Department of Physical Sciences, University of Oulu, Oulu, Finland, Jouni.Jussila@oulu.fi
(5) Space Environment Center, NOAA, 325 Broadway, Boulder, CO 80303, USA, David.S.Evans@noaa.gov
(6) AFRL, VSBXP, 29 Randolph Rd, Hanscom AFB, MA 01731-3010, USA, Frederick.Rich@hanscom.af.mil
(7) Geophys. Institute, Univ. Alaska, 903 Koyukuk Drive, Fairbanks, AK 99775-7320, USA, lumm@gi.alaska.edu

ABSTRACT

For moderately magnetically disturbed conditions, the EISCAT radar site near Tromsø, Norway, is located on the equatorial edge of the afternoon auroral oval for several hours, where energetic protons are a dominant particle energy source. A unique signature of proton precipitation is the Doppler-shifted H emissions. An imaging Echelle spectrograph designed for high spectral resolution studies of selected features located in the visible spectrum (including H_α and H_β) was deployed to identify and characterize proton precipitation at EISCAT during two winter-long campaigns in 2001-2002 and 2002-2003. Information on the overall auroral activity and on the cloud cover is provided by a large field-of-view conventional imaging spectrograph. We discuss a comprehensive set of combined optical, radar, and particle observations from these campaigns. Our ability to identify the type of precipitating energetic particles and to infer the ionospheric response is estimated from this dataset.

1. INTRODUCTION

During moderate magnetic activity (Kp=2-3), the European Incoherent SCATter (EISCAT) radar probing the high latitude ionosphere is situated for several hours at the equatorial edge of the afternoon auroral oval, where energetic protons are usually the dominant particle energy source [e.g., *Hardy et al.*, 1989]. *Senior et al.* [1991] compared the height-integrated conductivities derived from EISCAT data with those obtained from precipitating electrons. While there is agreement in the morning sector, the EISCAT-derived conductances are systematically larger than the electron-based model in the evening sector, suggesting ionization by energetic protons. Using simultaneous satellite- and ground-based observations from a satellite and the EISCAT radar, *Lilensten and Galand* [1998] have shown that protons are sometimes the major source of ionization above Tromsø. This result was confirmed by *Galand et al.* [2001], who used statistical patterns of both electron and ion

characteristics to assess the influence of proton precipitation on the Earth's auroral upper atmosphere.

When no simultaneous *in situ* particle data from satellite overpasses are available, the incoherent scatter radar can be used to detect the presence of particle precipitation, but it cannot identify the type of the incoming particles. Doppler-shifted H emissions are a unique signature of proton precipitation [*Eather*, 1967]. From the ground, H Balmer lines, H_α (656.3 nm) and H_β (486.1 nm), can be used to study proton precipitation [*Sigernes et al.*, 1996; *Lorentzen et al.*, 1998; *Lummerzheim and Galand*, 2001; *Lanchester et al.*, 2003; *Galand et al.*, 2003].

This paper compares a combined dataset of observations from the UHF EISCAT radar, from two optical spectrographs, and from particle detectors onboard low-altitude polar satellites. The ground-based radar and optical instruments were co-located near Tromsø, Norway (69.6ºN, 19.2ºE geographic and 66.4ºN, 103.4ºE geomagnetic coordinates). After a brief presentation of the various instruments used, the dataset is qualitatively compared during proton aurora and electron arcs. We then discuss the relevance of the optical observations and present a preliminary quantitative study of the ionospheric region perturbed by pure proton precipitation.

2. EISCAT UHF RADAR

The mainland EISCAT UHF radar is located near Tromsø, Norway, and transmits from a fully-steerable 32-m-diameter parabolic dish antenna within a 4-MHz-wide frequency band centerd on 928.5 MHz [*Folkestad et al.*, 1983]. Receiving may be done with the same antenna and with identical antennas in Kiruna, Sweden and Sodankylä, Finland, within a much wider frequency band. On the days studied here, the UHF radar was operated using the tau2 (Section 5.1) and arc1 (Section 5.2) data-taking programs with a peak output power of between 1.0 and 1.3 MW and with the antenna aligned along the geomagnetic zenith. In order to obtain good signal to noise ratio, the electron density

data derived from the radar observations are presented with a 1 min time and with 3 km at 100 km and 12 km at 180 km height resolution, respectively.

3. TWO IMAGING SPECTROGRAPHS

The two optical spectrographs, the Proton Aurora Context spectrograph (PAC) [*Baumgardner et al.*, 1993] and the High Throughput Imaging Echelle Spectrgraph (HiTIES) [*Chakrabarti et al.*, 2001], built at Boston University (BU), were deployed in the fall of 2001 at the EISCAT site. They successfully operated during two winter-long campaigns, from November 2001 to March 2002 and from October 2002 to April 2003. Their fields of view were confirmed to be centered at the magnetic zenith through the identification of stars and planets crossing the fields of view. The wavelength calibration was established using spectral lamps and was successfully validated through airglow features. A more comprehensive description of the optical instruments and of the data analysis can be found in *Galand et al.* [2003].

3.1 Proton Aurora Context Spectrograph

The PAC instrument consists of an imaging spectrograph covering the 350-800 nm spectral range [*Baumgardner et al.*, 1993]. It has a spectral dispersion of 1.2 nm/pixel, which is sufficient for a qualitative study on the state of the weather and the auroral activity. The 70º field of view is large enough to provide context information for the smaller field of view HiTIES observations. The exposure time was chosen to be 5 s to avoid saturation of the green and red lines. Sixteen images were co-added, so the integration time associated with each saved image is 80 s. The interval between two successive images is 2 min and 50 s, which includes a 1 min 30 s during which no data were recorded. The only photometric processing applied to the PAC data was the subtraction of the dark images and the correction for vignetting using flat images.

3.2 High Throughput Imaging Echelle Spectrograph

The HiTIES instrument was deployed to retrieve quantitative information on the proton aurora. It is a high spectral resolution (0.1 nm) imaging spectrograph capable of simultaneously observing multiple wavelengths in a wide spectral region from 390.0 to 770.0 nm [*Chakrabarti et al.*, 2001]. In the present paper, we concentrate on two of the four selected wavelength regions, in the vicinity of H_α (656.3 nm) and H_β (486.1 nm). The measured instrument full width at half maximum (FWHM) is 0.1 nm. The field of view associated with each spectral region is ~2º. The exposure time was chosen to be 4 min. The photometric calibration of HiTIES was performed using a C^{14} reference lamp and was validated through

the comparison of geocoronal /galactic H_α emissions. A similar instrument built at BU and operated by a group from the University of Southampton has successfully observed the proton aurora from Svalbard, Norway [*Lanchester et al.*, 2003]. The daytime variant of the HiTIES instrument has been successfully used to study OI (630.0 nm) from a sunlit aurora in conjunction with the Søndre Strømfjord incoherent scatter radar [*Pallamraju et al.*, 2001].

4. PARTICLE DETECTORS

The *in situ* electron and ion fluxes are provided by low altitude (~ 850 km) polar satellites: Defense Meteorology Satellite Program (DMSP) and National Oceanic and Atmospheric Administration (NOAA) / Polar Operational Environmental Satellites (POES). The DMSP/SSJ4 particle detectors look toward the local zenith and cover an energy range from ~ 50 eV to 30 keV in 20 channels [*Hardy et al.*, 1985; *Hardy et al.*, 1989]. The space environment monitor aboard the NOAA/POES satellites includes two instruments of interest here [*Fuller-Rowell and Evans*, 1987]. The Total Energy Detector (TED) covers an energy range from 50 eV (NOAA 15 and 17) and from 300 eV (NOAA 14) to 20 keV for electrons and positive ions. The Medium Energy Proton and Electron Detector (MEPED) extends from 30 keV over three integral energy bands for the electrons and from 30 keV to 2500 keV over four energy bands for the ions. All ions are assumed to be protons, as no ion composition information is available. Such an assumption is good at high latitudes during the moderately magnetic disturbed conditions studied here.

5. QUALITATIVE COMPARISON

5.1 Proton aurora

Fig.1 presents an overview of the dataset for the afternoon of December 3, 2002. Fig.1a shows the time history of the EISCAT electron density for two altitude levels. The *E* region around 115 km experienced a first increase in electron density (light shaded area) followed by a larger one (dark shaded area). A peak in electron density is seen around 16:45 UT at low altitude (~103 km), probably due to >10 keV electrons (vertical dotted line). Before using the optical data, we first checked the state of the weather by looking at the PAC 568.5 nm channel (Fig.1b). This channel is centered around the NaI triplet (568.263, 568.819 and 568.821 nm). These are anthropogenic emissions reaching the PAC field of view through tropospheric scattering and are indicator of cloudiness. The sky is cloudy between 16 and 17 UT and the optical data should not be used for any quantitative study. Unlike the other PAC channels presented here, no background was subtracted for the cloud monitoring channel. The

green line observed with PAC (Fig.1c) exhibits the two large increases (shaded areas) and the sharp peak (vertical dotted line) seen in the electron density history (Fig.1a). This confirms that all the enhancements observed are associated with particle precipitation. The PAC (Fig.1d) and HiTIES (Fig.1e) H_α channels, primarily sensitive to proton precipitation, only show the two large increases (shaded areas). These data suggest that the enhanced regions are produced by incident energetic protons, whereas the sharp peak around 16:45 UT is induced by hard (>10 keV) electron precipitation. In the auroral region, keV proton precipitation yields an ionization peak in the 110-125 km region [*Galand et al.*, 1999] consistent with the electron density data (Fig.1a). One could argue that the first large increase (light shaded area) is related to the state of the weather, as it closely follows the enhancement seen in the cloud monitoring channel (Fig. 1b). However, the high resolution H_α and H_β spectra acquired by HiTIES reveal the presence of broad Doppler-shifted profiles extending over more than 4 nm from 15:55 UT (similarly to those discussed by *Galand et al.* (2003)). This provides an indisputable proof of the presence of proton aurora in the field of view. During the time period of the light shaded area, DMSP 13, NOAA 14, and NOAA 15 were flying near the ground-based facilities (see Fig.1). The particle flux measurements from their particle detectors demonstrate that EISCAT was located at the equatorial edge of the auroral oval and was undergoing low (< 0.01 mW m^{-2}) particle precipitation with a predominance of energetic protons. As the Earth rotated, EISCAT moved further under the auroral oval, first encountering a significant proton precipitation. DMSP 14 crossed the magnetic latitude of EISCAT at 17:43 UT and detected a 0.22 mW m^{-2} proton flux below 30 keV. It encountered significant electron precipitation only at magnetic latitudes above 67.4°.

The peaks seen in the H_α channels around 15:45 UT in PAC (Fig.1d) and at 15:30 UT in HiTIES (Fig.1e) are produced by a bright (~300 R) HII region, the IC1396 nebula. Unlike the diffuse proton aurora, this feature is confined in space as observed by the two spectrographs. It is not seen in the PAC H_α data for an elevation angle 3° off the magnetic zenith (dashed line in Fig.1d). In addition, HiTIES H_α spectra show a narrow H_α line with a 0.2 nm FWHM, contrasting with the 2-3 nm FWHM found in the proton aurora. The time shift of the HII region between PAC (Fig.1d) and HiTIES (Fig.1e) is due to the curved slit in HiTIES inducing slightly non-parallel viewing directions between the two optical instruments. The H_α brightness derived from the HiTIES data is computed in two different ways, depending on the presence of proton aurora. When the only sources of H_α are galactic and geocoronal, the spectrum is narrow with an extent of

±0.2 nm (or less). It is integrated over a 0.4 nm range. When proton precipitation is observed, the profile is broad and the data are integrated over a larger spectral range (> 7 nm).

A similar analysis was undertaken for the afternoon of December 5, 2002 (Fig.2). The *E* region electron density in the 110-120 km range increased after 16:18 UT with a decrease around 17:11 UT (shaded areas in Fig.2a). The low altitude electron density around 103 km does not show any significant variation. The cloud monitoring channel (Fig.2b) has brightnesses of the same order as the clear sky level (defined by the horizontal dashed line). The PAC green line (Fig.2c), PAC H_α (Fig.2d), and HiTIES H_α (Fig.2e) brightness variations after 16:18 UT (shaded areas) are very similar to those seen in the 115 km EISCAT electron density (Fig.2a). Energetic protons start to precipitate after 16:18 UT and constitute the major ionization source of the ionosphere. This conclusion is corroborated by the presence of broad H_α and H_β Doppler profiles seen by HiTIES after 16:18 UT. The DMSP 13 and NOAA 14 satellites flew near EISCAT around 15:40-15:45 UT. Both indicate that, at that time the ground-based facility is equatorward of the auroral oval, the boundary of which is located above 69° magnetic latitude. At 17:15 UT, as the Earth rotated, EISCAT moved under the auroral oval and underwent pure proton precipitation carrying 0.12 mW m^{-2} below 30 keV, as attested by the particle data from DMSP 14. The electron aurora is encountered by DMSP 14, polarward of the proton aurora, above 67.1° magnetic latitude.

The PAC and HiTIES H_α brightnesses experienced an additional enhancement around 15:30 UT, which is not seen in the green line channel. This increase is associated with the IC1396 nebula, which has already been mentioned earlier. The appearance of this HII region on December 5 is 8 min 40 s earlier than on December 3. Keeping in mind the HiTIES (~4 min) and PAC (~3min) time resolution, this value agrees well with the expected shift of about 7 min 53 s (2 days*1 day/year*24 h/day*60 min/h/365 days/year).

5.2 Electron arcs

The *E* region ionosphere on November 7, 2002, was very perturbed between 18:00 and 20:20 UT and from 21:10 to 22:30 UT (Fig.3a). The peaks in the electron density history are most probably due to electron arcs. The PAC cloud monitoring channel (not shown here) was affected by the occurrence of the intense auroral activity. During such times, scattering inside the spectrograph generates an increase of the whole background level. However, during quiet times, such as between 20:30 and 21:10 UT, its brightness was at the clear sky level (as defined in Fig.1b and Fig.2b by the

dotted, horizontal line). The OI 557.7 nm green line (Fig.3b), the N_2^+ 1NG 427.8 nm (Fig.3c), and the OI 630.0 nm red line have brightnesses experiencing the same sharp increases as the E region electron density (Fig.3a). Overall, the peak times seen with PAC agree very well with the peak times in the electron density within the ~3 min PAC time resolution. Due to the 80 s time exposure of the PAC data, some double peaks seen in the EISCAT data appear as a single peak in the PAC data, such as around 18:18 UT, 19:00 UT, and 21:42 UT. The N_2^+ 427.8 nm channel is mainly sensitive to hard (>10 keV) electron precipitation. The two intense peaks near 22:00 UT and 22:15 UT seen in the EISCAT data at 106 km (Fig.3a) are clearly seen in the N_2^+ 427.8 nm channel, whereas the peaks occurring at higher altitudes, at 123 km, such as those at 20:00 UT and 21:20 UT, do not have clear correspondence in the N_2^+ 427.8 nm channel. DMSP 15 flew over an electron arc at 18:27 UT. Its electron detector saw an intense electron flux of 4 keV mean energy. They are expected to affect more the 123 km altitude level than the 106 km one, which agrees with the EISCAT data (Fig.3a). DMSP 14 crossed the magnetic latitude of EISCAT at 18:46 UT and saw electron precipitation with fluxes of one order of magnitude less than DMSP 15. Later, at 19:10 UT, NOAA 17 saw less than 0.3 mW m^{-2} electron flux below 20 keV, which agrees with the low electron density detected by EISCAT at that time. However, NOAA 17 particle instruments detected an electron flux of 3.1 mW m^{-2} while at 1° southward of EISCAT in magnetic latitude. This confirms the occurrence of strong electron arcs in this region of the auroral oval. At 20:51 UT, NOAA 17 sees again less than 0.3 mW m^{-2} electron flux below 20 keV at EISCAT magnetic latitude, which is too low to significantly disturb the ionosphere.

A similar study was undertaken for November 9, 2002, as illustrated in Fig.4. There is an excellent agreement between the times at which EISCAT electron density (Fig.4a) and PAC auroral brightnesses (Fig.4b-d) experience sharp peaks within the time resolution of the instruments. One exception is the intense peak seen by EISCAT at 23:24 UT, which does not appear in the PAC auroral brightnesses. This can be explained by the 1 min 30 s wait time underwent between two successive PAC images. The PAC cloud monitoring channel was at the level of clear sky outside the hard electron precipitation period, such as before 21:40 UT, between 22:40-22:50 UT, and after 1:30 UT. The clear sky conditions and electron arc activity were confirmed by the white-light TV measurements from the University of Oulu. No DMSP or NOAA satellites were flying near EISCAT during the period studied. The auroral activity on November 9, 2002, was observed by another set of optical instruments from the EISCAT site. This set operated by the University of Oulu included an auroral white-light TV-camera and a multi-channel photometer [*Jussila et al.*, 2003a] and was used to identify possible mechanisms of producing the observed auroral rays [*Jussila et al.*, 2003b].

6. DISCUSSION

The qualitative comparison between the EISCAT electron density, the PAC and HiTIES brightnesses and spectra, and the DMSP and NOAA particle fluxes attests to the capability of PAC and HiTIES spectrographs to detect the presence of proton precipitation and electron arcs, two significant sources of ionization in the high latitude ionosphere. The two spectrographs provide information on the particle type and characteristics crucial to interpret the EISCAT data. In proton aurora, the H$_\alpha$ enhancements correspond to similar variation in the electron density in the 110-120 km range. Other auroral lines, such as the green line and the N_2^+ 1NG 427.8 nm line, are also affected by proton precipitation, confirming earlier results [*Strickland et al.*, 1993, *Lummerzheim et al.*, 2001, *Galand et al.*, 2002]. In intense electron aurora, the time of occurrence of the auroral brightness peaks agrees well with those seen in the electron density within the time resolution of the instruments.

We have undertaken a preliminary quantitative study of this dataset for December 3, 2002. For that purpose, we used a combined electron and proton transport code [*Lummerzheim et al.*, 2001; *Galand et al.*, 2002]. We used the DMSP 14 ion flux at 17:43 UT as input of the model after adding a high energy tail based on NOAA17/MEPED observations from January 28, 2003 (18:30 UT, Kp=2). Even though the latter ones are from another day, they provide the best estimate available above 30 keV for the late afternoon sector. The derived total energy flux is 0.50 mW m^{-2} with a mean energy of 22.4 keV. We then computed the electron density and the auroral brightnesses and compared with the independent radar and optical data. Both the modeled and observed electron densities peak at 114.5 km reaching a value of 1.2 10^5 cm^{-3}. They agree within 16% over the 110-180 km range. This demonstrates that the energetic protons were the major energy source upon the ionosphere over EISCAT at that time. Both the modeled and HiTIES H Balmer spectra show broad, Doppler-shifted profiles, similarly to those observed by *Galand et al.* (2003). For H$_\alpha$, the synthetic and observed brightnesses peak at 228 R/nm and 115 R/nm, respectively, whereas, for H$_\beta$, they peak at 54 R/nm and 50 R/nm, respectively. The shapes of the modeled and measured profiles are in excellent agreement on the red-shifted side induced by the collisional angular redistribution [*Lummerzheim and Galand*, 2001]. The modeled blue-shifted wing is underestimated compared to the HiTIES observations. The discrepancies found in the brightnesses and

profiles can be explained by the uncertainties in the Balmer emission cross sections, especially above 3 keV where no laboratory data are currently available, the estimation of the extinction coefficient, and the contamination by nearby aurora.

7. ACKNOWLEDGEMENTS

8. REFERENCES

Baumgardner, J., B. Flynn, and M. Mendillo, Monochromatic imaging instrumentation for applications in aeronomy of the Earth and planets, *Opt. Eng.*, *32*, 3028-3032, 1993.

Chakrabarti, S., D. Pallamraju, J. Baumgardner, and J. Vaillancourt, HiTIES: A High Throughput Imaging Echelle Spectrograph for ground-based visible airglow and auroral studies, *J. Geophys. Res.*, *106*, 30,337-30,348, 2001.

Eather, R.H., Auroral proton precipitation and hydrogen emissions, *Rev. Geophys.*, *5*, 207-285, 1967.

Folkestad, K., T. Hagfors, and S. Westerlund, EISCAT: An updated description of technical characteristics and operational capabilities, *Radio Sci.*, *18*, 835-839, 1983.

Fuller-Rowell, T. J., and D. S. Evans, Height-integrated Pedersen and Hall conductivity patterns inferred from the TIROS-NOAA satellite data, *J. Geophys. Res.*, *92*, 7606-7618, 1987.

Galand M., R. Roble and D. Lummerzheim, Ionization by energetic protons in Thermosphere-Ionosphere Electrodynamics General Circulation Model, *J. Geophys. Res.*, *104*, 27,973-27,990, 1999.

Galand M., T.J. Fuller-Rowell, and M.V. Codrescu, Response of the upper atmosphere to auroral protons, *J. Geophys. Res.*, *106*, 127-139, 2001.

Galand M., D. Lummerzheim, A.W. Stephan, B.C. Bush, and S. Chakrabarti, Electron and proton aurora observed spectroscopically in the far ultraviolet, *J. Geophys.Res.*, *107*, DOI10.1029/2001JA000235, 2002.

Galand M., J. Baumgardner, D. Pallamraju, S. Chakrabarti, U.P. Løvhaug, D. Lummerzheim, B.S. Lanchester, M.H. Rees, Spectral imaging of proton aurora and twilight at Tromsø, Norway, submitted *to J. Geophys. Res.*, May 2003.

Hardy, D. A., M. S. Gussenhoven, and E. Holeman, A statistical model of auroral electron precipitation, *J. Geophys. Res.*, *90*, 4229-4248, 1985.

Hardy, D.A., M.S. Gussenhoven, and D. Brautigam, A statistical model of auroral ion precipitation, *J. Geophys. Res.*, *94*, 370-392, 1989.

Jussila, J. R. T., H. J. Holma, and K. U. Kaila, Optical auroral instrumentation of University of Oulu, *Proc. of 28th Annual Meeting on Atmospheric Studies by Optical Methods*, Sodankylä Geophysical Observatory Publications, *92*, 81-84, 2003a.

Jussila. J., H. Holma, K. Kaila, A. Aikio, P. Gallop, High-resolution EISCAT and optical observations of active rayed auroral arcs, submitted to *Ann. Geophys.*, 2003b.

Lanchester, B.S., M. Galand, S.C. Robertson, M.H. Rees, D. Lummerzheim, I. Furniss, L.M. Peticolas, H.U. Frey, J. Baumgardner, and M. Mendillo, High resolution measurements and modeling of auroral hydrogen emission line profiles, *Ann. Geophys.*, *21*, 1629-1643, 2003.

Lilensten J. and M. Galand, Proton/electron precipitation effects on the electron production and density above EISCAT and ESR, *Ann. Geophys., 16*, 1299-1307, 1998.

Lorentzen, D.A., F. Sigernes, and C.S. Deehr, Modeling and observations of dayside auroral hydrogen emission Doppler profiles, *J. Geophys. Res.*, *103*, 17,479-17,488, 1998.

Lummerzheim D., and M. Galand, The profile of the hydrogen H_β emission line in proton aurora, *J. Geophys. Res.*, *106*, 23-31, 2001.

Lummerzheim D., M. Galand, J. Semeter, M.J. Mendillo, M.H. Rees, and F.J. Rich, Emission of OI(630 nm) in proton aurora, *J. Geophys. Res.*, *106*, 141-148, 2001.

Pallamraju, D., J. Baumgardner, S. Chakrabarti, and T.R. Pedersen, Simultaneous ground-based observations of an auroral arc in daytime OI 630.0 nm emission and by Incoherent Scatter Radar, *J. Geophys. Res.*, *106*, 5543-5549, 2001.

Senior, C., Solar and particle contributions to auroral height-integrated conductivities from EISCAT data: A statistical study, Ann. Geophys., *9*, 449-460, 1991.

Sigernes, F., G. Fasel, J. Minow, C.S. Deehr, R.W. Smith, D.A. Lorentzen, L.T. Wetjen, and K. Henriksen, Calculations and ground-based observations of pulsed proton events in the dayside aurora, *J. Atmos. Terr. Phys.*, *58*, 1281-1291, 1996.

Strickland, D. J., R. E. Daniell, Jr., J. R. Jasperse, and B. Basu, Transport-theoretic model for the electron-proton-hydrogen atom aurora, 2. Model results, J. Geophys. Res., 98, 21533-21548, 1993.
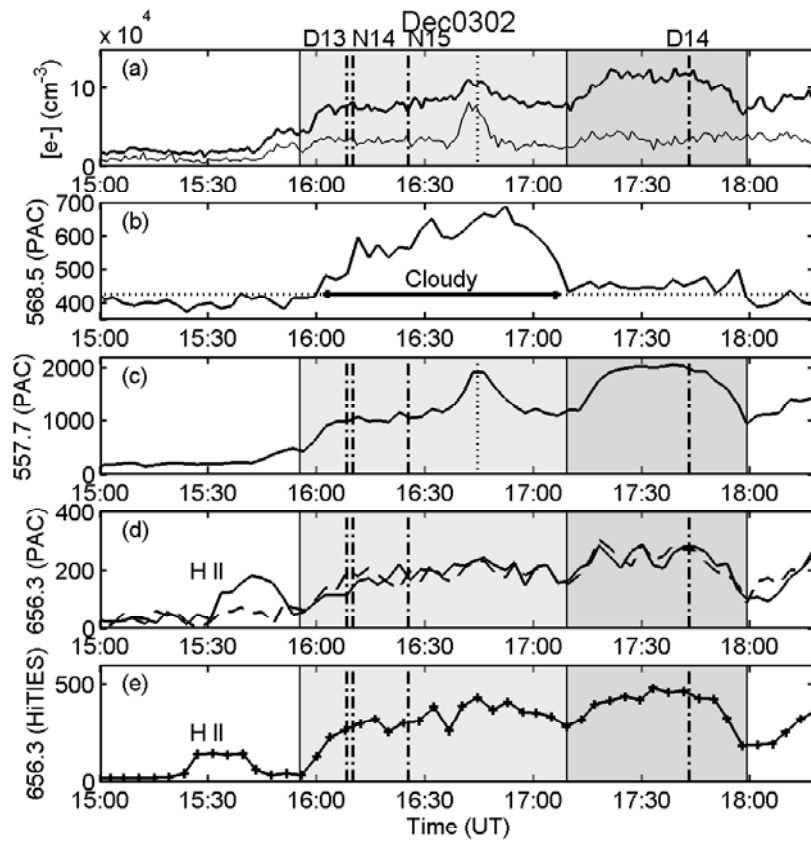
Fig. 1. Overview of the dataset for December 3, 2002. The planetary geomagnetic Kp index was equal to 3 during this time period. The different panels show the time history plots of: **(a)** the electron density from the EISCAT radar for an altitude range of 100-106 km (thin line) and 110-120 km (thick line), **(b)** PAC cloud monitoring channel at 568.5 nm, **(c)** PAC green line channel at 557.7 nm, **(d)** PAC H$_\alpha$ Balmer channel at 6563 nm for two viewing angles at 77.8° (magnetic zenith) in solid line, and at 80.7° in dashed line, **(e)** HiTIES H$_\alpha$ Balmer line in Rayleigh. All the data are for magnetic zenith viewing, except as otherwise specified. The optical data extracted are valid for a field of view of ~2°. The dashed dotted horizontal line in **(b)** represents the mean level for a clear sky. The y-axis associated with PAC data in **(b)-(d)** are in relative brightness. The shaded areas represent periods of proton precipitation. The vertical lines indicate times related to the presence of hard (>10keV) precipitation in the field of view (dotted line), and times of near flybys by DMSP (D13, D14) or NOAA (N14, N15) satellites (dashed-dotted lines).
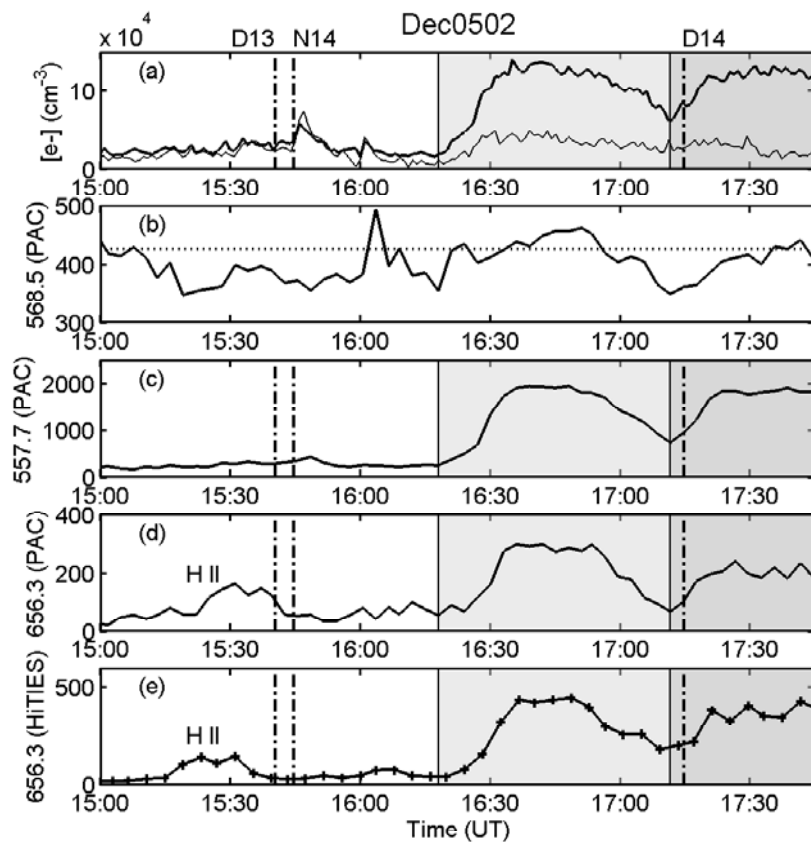

Fig. 2. Same as Fig.1, but for December 5, 2002. The planetary geomagnetic Kp index was equal to 3 during this time period. All the data are for magnetic zenith viewing.
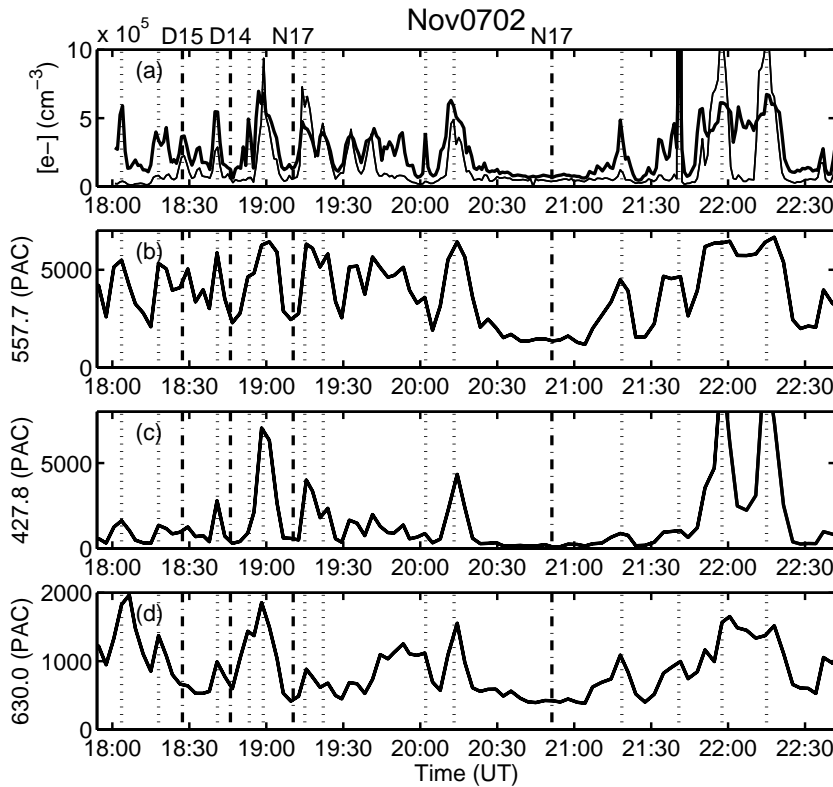
Fig. 3. Overview of the ground-based data for November 7, 2002. The planetary geomagnetic Kp index was equal to 3 during this time period. The different panels show the history plots of: **(a)** the electron density from the EISCAT radar for an altitude of 106 km (thin line) and 123 km (thick line), **(b)** PAC green line channel at 557.7 nm, **(c)** PAC N_2^+1NG channel at 427.8 nm, **(d)** PAC red line channel at 630.0 nm.

All the data are for magnetic zenith viewing. The y-axis associated with PAC data in **(b)-(d)** are in relative brightness. The vertical lines indicate times related to the presence of an electron arc in the field of view (dotted line) and times of near flybys by DMSP (D14, D15) or NOAA (N17) satellites (dashed-dotted lines).
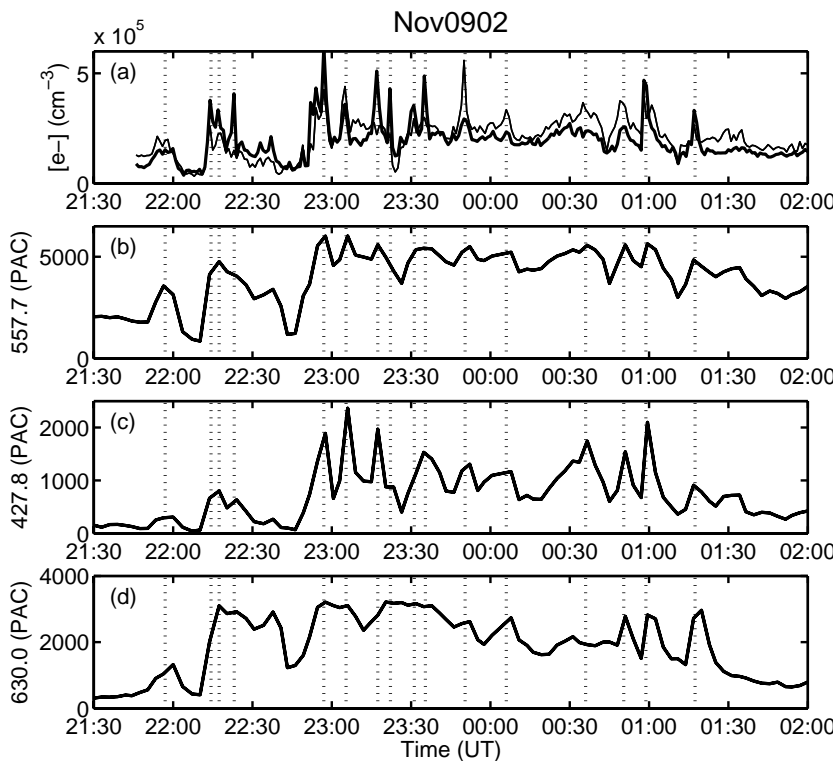

Fig. 4. Same as Fig.3, but for November 9, 2002. The planetary geomagnetic Kp index was equal to 3 during this time period. Panel **(a)** shows the electron density from the EISCAT radar for an altitude of 123 km (thin line) and 165 km (thick line).